Prime Mover and Energy Storage Considerations for a Hydrogen-Powered Series Hybrid Shuttle Bus

M. M. Flynn[1], C. S. Hearn[1], M. C. Lewis[1], R. C. Thompson[1], R. G. Longoria[2]

[1]Center for Electromechanics
University of Texas
1 University Station, R7000
Austin, TX 78712

[2]Mechanical Engineering Dept.
University of Texas
1 University Station, C2200
Austin, TX 78712

***Abstract*-This paper describes simulation results obtained through modeling the operation of a 6.7 m long hydrogen-powered shuttle bus. The actual shuttle bus and its hydrogen refueling station constitute the first of its kind in the state of Texas. The simulations are used to initially verify the stated performance of the shuttle bus and to validate the modeling approach. The vehicle model is then modified to assess the predicted changes in performance, efficiency, and route following capability while conducting a parametric study involving fuel cell and internal combustion prime movers as well as chemical battery and flywheel energy storage systems. Simulation results show that a fuel cell-powered shuttle bus with a high power density, low mass energy storage system provides the highest vehicle range and lowest energy consumption.**

I. Introduction

U.S. Environmental Protection Agency reports show that internal combustion engine-powered vehicles using hydro-carbon fuels account for 75 % of national carbon monoxide emissions, 45 % of nitrous oxide emissions, and nearly 40 % of the volatile organic compound emissions [1]. Larger vehicles such as urban transit buses can be among the worst offenders; however, buses that consume a non-hydrocarbon fuel such as hydrogen can achieve ultra low or even zero emissions with a simultaneous 30 – 66 % reduction in fuel usage compared to conventional diesel powered buses [2, 3, 4].

To further the research and development of such low emissions buses, the University of Texas at Austin and the Gas Technology Institute have entered into a collaborative agreement to bring the first hydrogen vehicle fleet and refueling station to the State of Texas. The partnership's mission is to create an advanced transportation and fueling infrastructure which strengthens the research community's capabilities with regard to emerging and advanced hydrogen propulsion technologies. As an initial step towards this goal, a fuel cell powered 6.7 m long plug in hybrid shuttle bus has been acquired for demonstration, evaluation, and performance testing.

This paper provides the results of computer simulations of the shuttle bus over an urban transit route as well as the performance of the actual vehicle for comparison and model validation. The simulations are then leveraged to evaluate the performance of the bus while using various prime mover and energy storage combinations.

Prime mover variants include a polymer electrolyte membrane (PEM) fuel cell and a hydrogen-fueled internal combustion engine. Energy storage alternates consist of two relative extremes among the vast array of storage solutions. Specifically, a nickel cadmium (NiCd) chemical battery pack which is installed on the actual vehicle is modeled and represents a relatively high specific energy but low specific power option. Additionally, a high-speed flywheel-based system is modeled representing a relatively high specific power but low specific energy storage solution. The details of the shuttle bus components and their advantages and disadvantages are discussed in the following sections.

II. Shuttle Bus Overview

The shuttle bus discussed in this paper is shown in Fig. 1. The bus is a 6.7 m long plug-in series hybrid using NiCd batteries for energy storage and a PEM fuel cell for range extension. The rated gross vehicle weight (GVWR) is 8845 kg which includes 22 seated and 10 standing passengers. The vehicle has a maximum speed of 20 m/s and is designed for transport within highly urban areas. For propulsion the bus employs a 75 kW continuous power induction motor coupled to a gear reducer, drive shaft, and differential to drive the rear wheels. Table I provides a summary of the shuttle's specifications and performance; the performance values will be compared against the simulation results for validation of the model.

Figure 1 Fuel cell shuttle bus modeled in simulations

TABLE I
SHUTTLE BUS SPECIFICATIONS AND PERFORMANCE SUMMARY

Parameter	Value	Unit
Vehicle		
Length	6.7	m
GVWR	8845	kg
Passengers	32	
Propulsion Motor Continuous Power	75	kW
Propulsion Motor Peak Power	100	kW
Air Conditioner Power at Full Output	5.5	kW
Range at GVWR, Batteries Only* (no air conditioner usage)	72	km
Maximum Speed	20	m/s
Range at GVWR, with Fuel Cell* (no air conditioner usage)	400	km
Range at GVWR, with Fuel Cell* (with air conditioner usage)	305	km
Energy Consumption* (no air conditioner usage)	0.62	kWh/km
Energy Consumption* (with air conditioner usage)	1.06	kWh/km
Battery		
Type	NiCd	
Stored Energy	60	kWh
Usable Energy	48	kWh
Depth of Discharge	80	%
Battery Modules per Bank	50	
Battery Banks	2	
Total Battery System Mass	3175	kg
Fuel Cell		
Type	PEM	
Power Rating	19.1	kW
Power Response Time Constant	4	s
Hydrogen Storage	16	kg
Storage Pressure	34.5	MPa
Fuel Cell and Balance of Plant Mass	136	kg

* Range and energy consumption are dependent on road conditions, air conditioner usage and operator proficiency

The NiCd battery energy storage is composed of 100 battery modules divided into 2 banks. The total stored energy is 60 kWh; allowable depth of discharge is 80 % providing a usable energy of 48 kWh. The nominal output voltage of a given battery bank is 300 V. NiCd batteries were selected versus other battery technologies such as nickel metal hydride (NiMH) or lithium ion (Li-ion) for two primary reasons. First, NiCd batteries offer long life under high cycling operation with a large depth of discharge. Second, NiCd batteries are among the most mature and are therefore relatively inexpensive (e.g. 40 % the cost of suitable NiMH batteries). Vehicle range using the batteries only is limited to 72 km depending on road conditions and air conditioner usage.

The PEM fuel cell develops a maximum power of 19.1 kW and draws hydrogen from 2 roof mounted tanks pressurized to 34.5 MPa storing a total 16 kg of hydrogen. The hydrogen provides an additional 200 kWh of useable energy storage and increases the bus's range to a maximum of 400 km depending on road conditions and air conditioner usage.

III. OVERVIEW OF SIMULATION TECHNIQUE

A. *Simulation Overview and Route Selection*

A computer model of the shuttle bus was created using the simulation software package Powertrain Simulation Analysis Toolkit (PSAT) developed by Argonne National Laboratories. PSAT is a forward-looking simulation tool that enables the construction and analysis of detailed vehicle models and control systems by integrating the capabilities of Matlab, Simulink, Stateflow, and a graphical user interface.

For all vehicle simulations a common route termed the "PRC Campus Route" was used and is displayed in Fig. 2. This route represents a transportation link the shuttle bus will provide between the host research campus and a nearby commercial district during an initial evaluation and demonstration phase. The route is 4.84 km long repeated on a 15 minute basis with an average speed of 4.5 m/s. Maximum acceleration and deceleration is 0.9 m/s^2 and 1.9 m/s^2 respectively. The shuttle is stopped for 37.4 % of the route duration. Daily service is intended to be for 10 hours requiring the shuttle to complete 194 km.

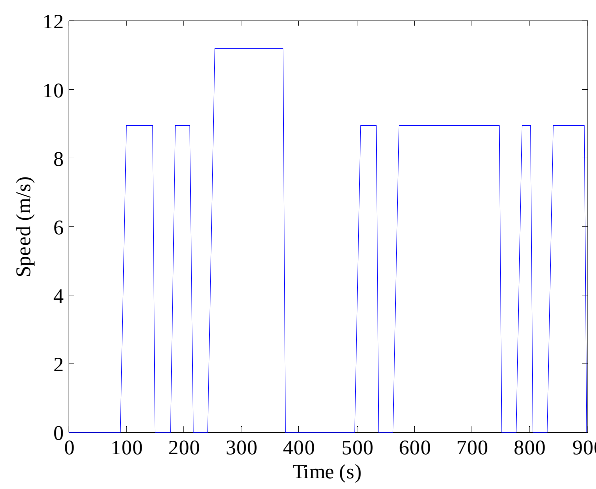

Figure 2. PRC Campus Route used for shuttle bus simulations

B. *Shuttle Bus Architecture as Constructed*

The powertrain and auxiliary component architecture of the shuttle as constructed is shown in Fig. 3. The propulsion motor's mechanical power is delivered to the wheels via a two-stage gear reduction indicated by the 'torque coupling' and 'differential' blocks in the figure. The 'wheel' block

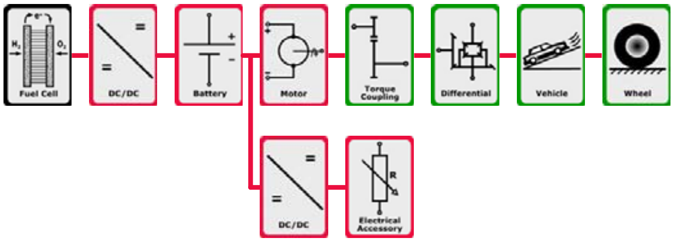

Figure 3. Shuttle bus architecture as constructed

accounts for mechanical braking and rolling friction losses, while the 'vehicle' block models aerodynamic losses.

The 'electrical accessory' block models items such as lights, pumps, and the air conditioner which is set to be on continuously during the simulations. Total electrical accessory load is 6.3 kW.

The fuel cell is controlled in such a manner as to supply the entire 6.3 kW of electrical accessory load; the remaining 12.8 kW of generation capability is used to supply the fuel cell's balance of plant losses and the propulsion motor demand if required. During minimal propulsion motor power demand, excess fuel cell power is diverted to charge the batteries. In this manner the fuel cell, which is a slow responding device, can be controlled to operate at a constant power level. The fuel cell is commanded to reduce power from maximum only if the batteries are above a target state of charge, typically 95 %.

The batteries are used to provide the remaining power demanded by the propulsion motor not supplied by the fuel cell and to capture regenerated braking energy.

C. Description of Prime Movers Used in Simulations

Two hydrogen-fueled prime movers were modeled for use in the simulations discussed below. The first model is that of the PEM fuel cell delivered with the actual shuttle bus. The second is a hydrogen-fueled internal combustion engine. Some relative advantages and disadvantages of each technology are discussed below.

1) PEM Fuel Cell: This device was selected for modeling because simulating the vehicle as constructed allows for validation of the simulation through correlation with future empirical data, and also because fuel cells represent the highest efficiency hydrogen-powered prime mover technology available with full-power values in the range of 45 to 55 % [4]. Partially loaded efficiencies are typically higher, often above 60 %. In addition, the fuel cell allows the shuttle bus to achieve essentially zero harmful emissions at the vehicle.

These benefits come with a high cost and some significant disadvantages. For example, fuel cells are comparably very expensive, with a typical pricing figure of $3000/kW; much of this cost results from the use of the platinum catalyst [5]. PEM fuel cells have a high sensitivity to carbon monoxide which bonds to the anode and thus reduces power output capability. Studies have shown power capability can be reduced by 10 % after as little as 7000 km of use, and lifetimes are typically only a few thousand hours [6]. Power consumed by auxiliary systems used to ensure proper electrolyte membrane moistness increase system complexity, volume, and mass while reducing system efficiency. PEM fuel cells must never be allowed to freeze since ice formation within the cell will cause damage to the membrane and reduce power output according to the size of the affected area. Lastly, PEM fuel cells respond slowly to power command changes. Typical time constants for power output changes are on the order of 4 seconds.

2) Hydrogen-Powered Internal Combustion Engine: The second prime mover modeled is a hydrogen-powered internal combustion engine (H_2ICE). Compared to a PEM fuel cell, an H_2ICE is a more robust, less expensive option yet has reduced efficiency. This technology is also more mature and is poised for mass production by some automakers [7].

Thermal efficiencies for naturally aspirated H_2ICEs have been reported around 38% which is somewhat higher than conventional gasoline engines [8]. H_2ICEs can operate with near zero emissions at the vehicle. The main sources of emissions are nitrogen oxides (NO_x) which can be controlled by either running the engine lean or operating at stoichiometric conditions with a post catalytic converter [9,10]. The only source of hydrocarbon emissions comes from lubricating oils used in the engine.

Compared to conventional gasoline spark ignition engines, power densities of naturally aspirated H_2ICEs are reduced due to the low density of hydrogen which displaces about 30% the volume of air in the cylinders. This reduction in power can be counteracted by operating at higher compression ratios, pressure boosting, and direct injection to meet and exceed power densities of naturally aspirated gasoline engines [11, 12]. Due to the low ignition energy of hydrogen, pre-ignition will limit the torque output and performance of an H_2ICE. Control strategies for pre-ignition include using cold-rated spark plugs, water injection systems, and lower coolant temperatures to reduce in cylinder temperatures and hot-spots [9,13].

The H_2ICE engine model used within PSAT is based on tests conducted by Sandia National Laboratories on a single cylinder H_2ICE which report an efficiency that is 90 % of an equivalent diesel engine. The engine model was thus based on a diesel engine and scaled to replicate performance characteristics obtained for a 2.0 liter Ford Zetec engine fueled by hydrogen [8]. This engine is a naturally aspirated inline 4 cylinder engine operating at a 14.5:1 compression ratio. Power output is 23.4 kW at 2,500 r/min.

An advantage of the H_2ICE is that is can be used to mechanically drive the vehicle wheels and can thus be used in more than just series hybrid configurations. However, doing so without on-board energy storage requires a much larger engine than the one modeled and will have a commensurate increase in hydrogen consumption. Since stored hydrogen on the shuttle is limited to 16 kg and since it is desirable to ensure prime mover powers are comparable for meaningful comparisons, a similarly power rated H_2ICE was chosen. It should be noted that in order to interface with the vehicle's electric propulsion motor, the mechanical output of the engine must be coupled to a generator which results in an additional efficiency reduction for the engine-generator combination.

D. Description of Energy Storage Used in Simulations

Two forms of energy storage were used in the simulations to model systems with widely differing characteristics. The first system is composed of the NiCd battery modules which are installed on the vehicle as constructed. The second storage device is a prototype high-speed flywheel system. Both devices are discussed below.

1) NiCd Batteries: One hundred NiCd batteries are modeled in two battery banks in the simulations. The banks provide a relatively high specific energy (18.9 Wh/kg) storage system while offering a lifetime of more than 2,000 cycles with an 80 % depth of discharge. The usable energy of 48 kWh allows the shuttle bus to be a battery dominant hybrid and use the fuel cell as a range extension device. This in turn allows the propulsion motor to derive its energy needs primarily from the batteries while the comparably less powerful fuel cell performs the role of a battery charger.

Disadvantages of the NiCd battery banks include a relatively low specific power (63.0 W/kg), a high mass of 3175 kg (36 % of the shuttle's GVWR), and the use of cadmium which is not environmentally friendly. Another concern is the safety hazard that exists when working around a high voltage battery bank, since it remains lethal even when discharged. Lastly, even though NiCd batteries do offer excellent cycle-ability and long life compared to other battery technologies, these life-related values are low compared to flywheel systems.

2) High-speed flywheel system: An 18,000 r/min flywheel system has been designed for the simulations and is detailed in [14]. The flywheel shown in Fig. 4 uses a 120 kW, 3-phase, inside-out, permanent magnet motor to spin a steel arbor with a carbon composite rim in a vacuum on rolling element bearings. Total stored energy is 1.25 kWh; however, in operation the maximum depth of discharge is controlled to be 75 % allowing for a usable energy of 0.94 kWh. While the flywheel is structurally designed for a much longer cycle life, the bearings require replacement after 10 years of use (i.e. 70,000 hours of operation).

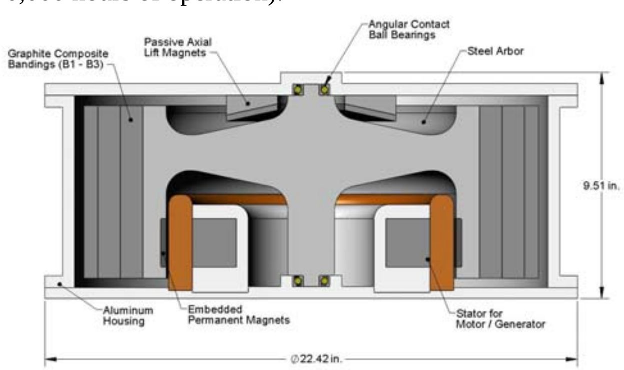

Figure 4. Cutaway view of flywheel motor and arbor used in simulations

The mass of the flywheel system is 432 kg yielding a higher specific power compared to the NiCd system of 277.8 W/kg but a significantly lower specific energy of 2.9 Wh/kg. When 20 kg of auxiliary systems are included, the flywheel system mass is 2723 kg less than the NiCd system. This mass savings greatly reduces the shuttle's energy and power requirements.

A major benefit of the flywheel system centers on its power and energy stability over its lifetime. Specifically, in contrast to the NiCd system, the flywheel experiences no degradation in its stored energy or power output capability over its lifetime which is intended to be at least as long as the host vehicle itself. Moreover, maintenance during this lifetime is limited to infrequent bearing replacements and auxiliary system service. It is important to note, that unlike the NiCd system, the flywheel can be easily and quickly discharged which alleviates any potential electrical hazards from the system during vehicle service.

Flywheel system disadvantages are twofold. First, compared to the NiCd system stored energy is low. However, as will be highlighted by the simulations that follow, the reduced mass of the flywheel system reduces this requirement greatly. A notable exception would be during prolonged hill climbing in which the limited energy reserve of the flywheel system and the relatively small prime mover power rating result in a low gradeability.

The second disadvantage compared to the NiCd system concerns the kinetic form of energy storage. While the designed safety margins are sufficient to ensure safe long-term operation, the dynamics of automobile crashes necessitates the prudent designer to employ a containment system. This system accounts for 235 kg, or 54 % of the flywheel mass. A gimbal system is also used to provide long bearing life which accounts for 44 kg of the flywheel mass.

IV. Fuel Cell-Battery Shuttle Bus Simulation

The shuttle bus was simulated as constructed to form a baseline for subsequent simulation comparisons and to compare the results to the actual shuttle bus performance. The vehicle architecture as simulated was provided in Fig. 3. During the simulation, the fuel cell provides power for accessory loads at all times and for the propulsion motor during acceleration. When propulsion power is minimal, the fuel cell diverts excess power output to the batteries in an attempt to maintain a 95 % state of charge target. When the hydrogen storage is exhausted, the shuttle maintains a limited battery-only range. The batteries provide any propulsion motor power not available from the fuel cell.

Fig. 5 shows the route following performance of the fuel cell-battery shuttle bus by comparing the commanded vehicle speed to the simulation result. The very low average tracking error of 0.013 m/s and maximum error of 0.39 m/s show that the shuttle is able to follow the route without difficulty.

Fig. 6 presents the fuel cell and battery output powers as well as the motor input power (note that for clarity, offsets for the time axes in this paper have been set to zero). It can be seen that the fuel cell and battery work in conjunction to provide the required motor power. Additionally, when the motor power request is zero the fuel cell can been observed to be recharging the battery. At a time of about 115 s, the fuel cell's output power is reduced to support the electrical accessory load only since the battery has been recharged to its target value of 95 %.

The battery state of charge is shown in Fig. 7 wherein the shuttle has just begun the route; the batteries are initially 100 % charged and are maintained at the target value by the fuel cell. The shuttle can maintain the state of charge until the hydrogen supply is exhausted at a distance of 298 km. The shuttle can continue operating for another 49 km in a battery-only mode before reaching the maximum depth of discharge of 80 %. The total vehicle range is 347 km, significantly more than the 194 km required.

The simulation yielded an energy efficiency value of 1.78 kWh/km which is higher than the manufacturer's datum provided in Table I. However, the manufacturer's efficiency data are average values tabulated from end users and are highly route dependent. To further investigate the model, an additional simulation was performed wherein the shuttle bus was driven fully-loaded at a constant speed of 18 m/s. The energy efficiency was determined to be 0.89 kWh/km which is well within the range provided in Table I. It is thus concluded that while the PRC-Campus route is more severe in terms of energy usage than the average user route compiled by the manufacturer, the model accurately represents the shuttle bus.

The manufacturer's reference for acceleration time from zero to 11.2 m/s is 14 seconds. This compares well with the simulation result of 13.2 seconds (5.7 % error). Overall, acceleration time and energy usage results provide sufficient confidence in the shuttle model to proceed.

V. Fuel Cell-Flywheel Shuttle Bus Simulation

For the second simulation the two battery banks were replaced with the flywheel system described above, the vehicle mass thus reduces to 6122 kg. Overall vehicle architecture remains the same as shown in Fig. 3. The flywheels are controlled in a similar manner as the battery banks with the exception that the target state of charge is 80 %. This lower value allows sufficient headroom for capturing re-generated energy while simultaneously increasing bearing life.

The route following performance of the fuel cell-flywheel shuttle is excellent with an average error of 0.001 m/s and a maximum error of 0.09 m/s. Fig. 8 shows the fuel cell and flywheel output powers and the propulsion motor input power. Compared to the fuel cell-battery shuttle, the lighter weight of the flywheel system permits the fuel cell-flywheel shuttle to accelerate with 30 % less power thus requiring less energy from the storage system. The reduced energy use in turn allows the flywheel to be recharged faster and therefore reduces the fuel cell average power output and fuel consumption.

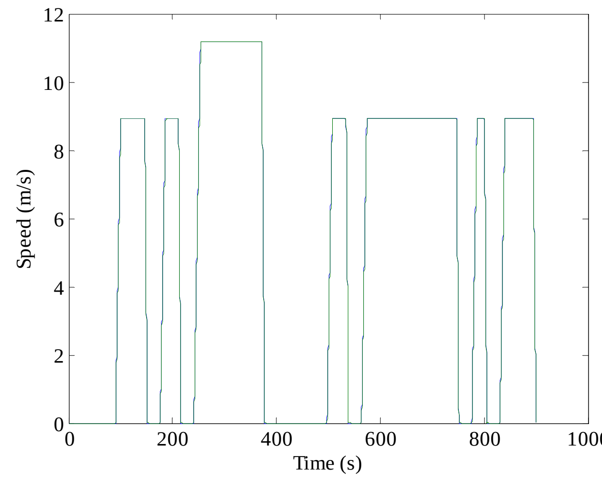

Figure 5. Comparison of commanded versus vehicle speed

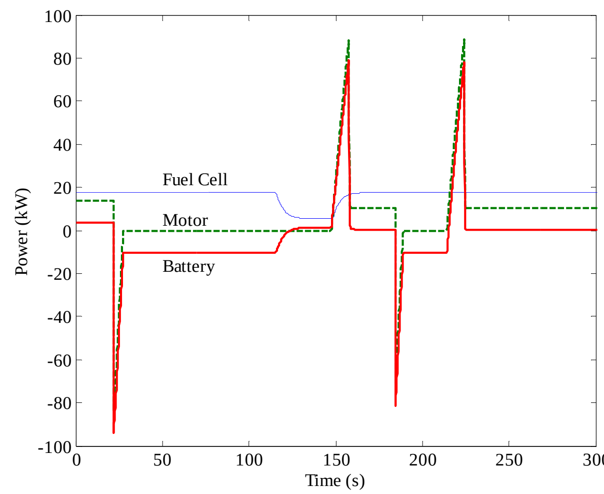

Figure 6. Fuel cell-battery shuttle bus powers

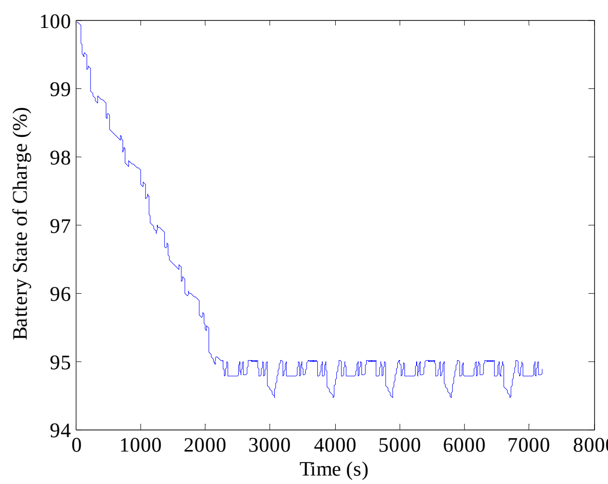

Figure 7. Battery state of charge during initial use of shuttle

The flywheel system has a higher efficiency than the battery banks, especially at peak power usage. For instance the average two-way efficiency of the flywheel system is 84.6 % compared to only 70.3 % for the batteries. The improved efficiency combined with the reduced energy transfer requirements afforded by the lighter weight of the flywheel system allows a higher percentage of the regenerated braking energy to be captured. For example, the fuel cell-flywheel shuttle is able to recuperate 69.9 % of the recoverable braking energy compared to only 48.7 % for the battery equipped shuttle. Recoverable braking energy is defined as the kinetic energy of the shuttle minus rolling friction and aerodynamic losses.

The flywheel system's state of charge and corresponding speed are shown in Fig. 9. The higher efficiency and lighter weight of the flywheel system results in an improved vehicle energy efficiency of 1.43 kWh/km. Range is improved to 370 km before the hydrogen supply is exhausted with an additional 2.2 km using the flywheel alone. Acceleration time from 0 to 11.2 m/s is improved to 8.9 s.

VI. H_2ICE-Battery Shuttle Bus Simulation

The H_2ICE-battery shuttle architecture is shown in Fig. 10. The 136 kg fuel cell from the previous models has been replaced with a 120 kg H_2ICE and a 44 kg, 30 kW generator. The vehicle mass as simulated is 8873 kg reflecting a net mass increase of 28 kg which is considered insignificant.

During the simulation, the engine is controlled to turn on only when the battery state of charge falls below 80 %. When the state of charge reaches 85 % the engine is turned off. When the engine is on, it is available to help support the electrical accessory and propulsion loads as well as recharge the battery. When the engine is off, all loads are supplied by the batteries including the electrical accessories.

Unlike fuel cells which are more efficient when partially loaded, the H_2ICE is most efficient at maximum torque production which occurs at a single operating speed. Thus while the engine is on, it is run at the single speed of 2,500 r/min with a resultant output torque of 89.4 Nm and an efficiency of 37 %.

Route tracking performance is comparable to the similarly massive fuel cell-battery shuttle with an average speed error of 0.013 m/s and a maximum speed error of 0.48 m/s. The generator and battery output powers along with the propulsion motor input power are shown in Fig. 11. At a time of approximately 130 seconds, the engine is started to recharge the battery and assists the battery with the propulsion and electrical accessory loads. The battery state of charge for the first 29 km of operation is shown in Fig. 12 in which the engine turn on and turn off events are evident.

Energy efficiency is worse compared to the previously discussed fuel cell-based shuttles due to the lower prime mover efficiency. The vehicle energy requirement is 2.37 kWh/km, which affords a range of 225 km while hydrogen is available, plus an additional 39 km during a battery-only mode.

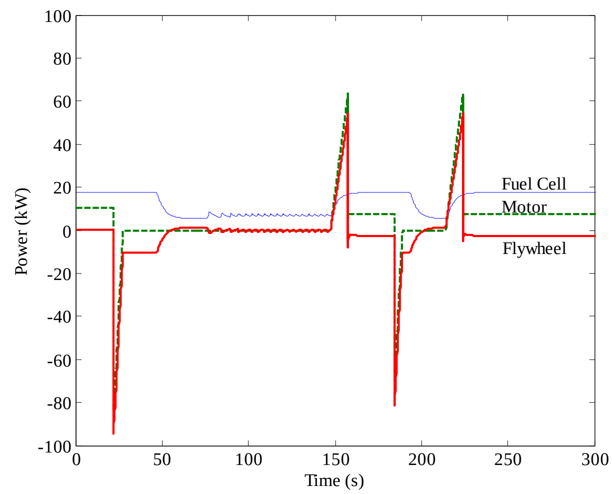

Figure 8. Fuel cell-flywheel shuttle bus powers

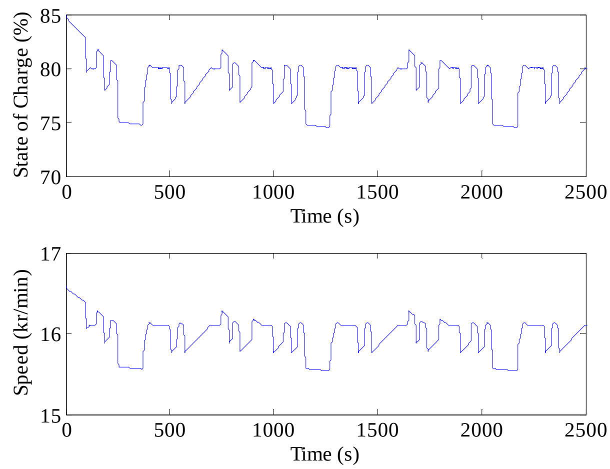

Figure 9. Flywheel state of charge and speed for fuel cell-flywheel shuttle

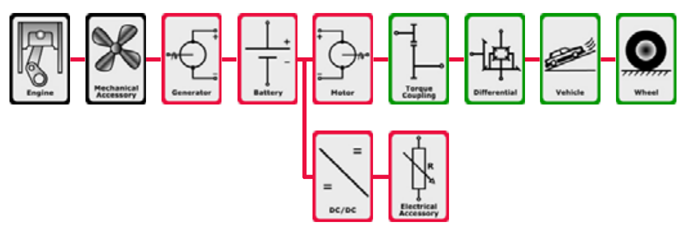

Figure 10. H_2ICE-battery shuttle bus architecture

Acceleration time from zero to 11.2 m/s is 13.2 s. This is so despite the fact that the H_2ICE is more powerful than the fuel cell since traction power is limited by the propulsion motor.

VII. H_2ICE-Flywheel Shuttle Bus Simulation

The architecture of the H_2ICE-Flywheel shuttle bus is similar to that shown in Fig. 10 except the battery is replaced with the flywheel system. Additionally, the engine is controlled in the same manner as described above except it is turned on when the flywheel state of charge falls below 70 %

and turned off when the state of charge is above 85 %. This wider range prevents the engine from cycling too often.

The vehicle mass as simulated is 6150 kg which is 28 kg more than the fuel cell-flywheel shuttle. Route following capability was excellent with an average speed error of 0.001 m/s and a maximum speed error of 0.09 m/s. Flywheel and generator output powers and the propulsion motor input power are shown in Fig. 13. Flywheel state of charge and the corresponding speed are shown in Fig. 14. These figures show that the powertrain behavior of the flywheel equipped shuttle is similar to that of the battery based shuttle with the exception that the engine cycles more often with the flywheel system due to its lesser energy storage.

The higher efficiency of the flywheel storage system and lighter weight of the engine-flywheel shuttle resulted in improved performance compared to the engine-battery shuttle. For example, vehicle efficiency improved to 1.94 kWh/km; range increased to 275 km with hydrogen plus 2.1 km using the flywheel only; and acceleration time to 11.2 m/s was reduced to 8.9 s which is similar to the fuel cell-battery shuttle as expected. Lastly, the H_2ICE-flywheel shuttle was able to recuperate 69.6 % of the recoverable braking energy compared to only 48.6 % for the H_2ICE-battery shuttle.

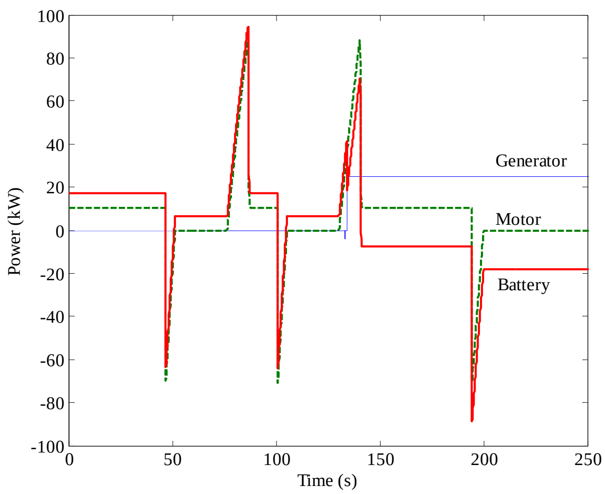

Figure 11. H_2ICE-battery shuttle bus powers

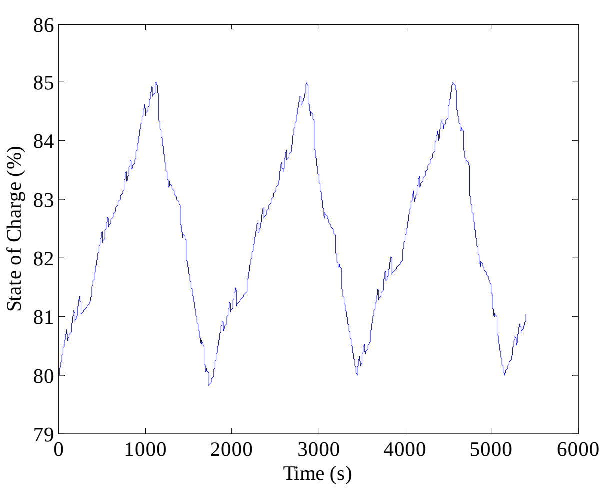

Figure 12. Battery state of charge for H_2ICE-battery shuttle

VIII. CONCLUSION

Four shuttle bus configurations have been compared and are summarized in Table II. Among these, the two that utilized a fuel cell as the prime mover achieved the best vehicle efficiency and range. This is to be expected as the fuel cell's efficiency is greater than the combined engine-generator efficiency. However, in cases where the performance of the H_2ICE equipped shuttle is acceptable, it affords significant cost savings, improved robustness, and longevity as discussed above.

For the route simulated, the flywheel energy storage system resulted in improved performance and efficiency compared to the battery storage system. This is largely due to the fact that the lower power density of the battery system necessitates a storage system design that is oversized in terms of stored energy in order to achieve the desired power capability. Thus,

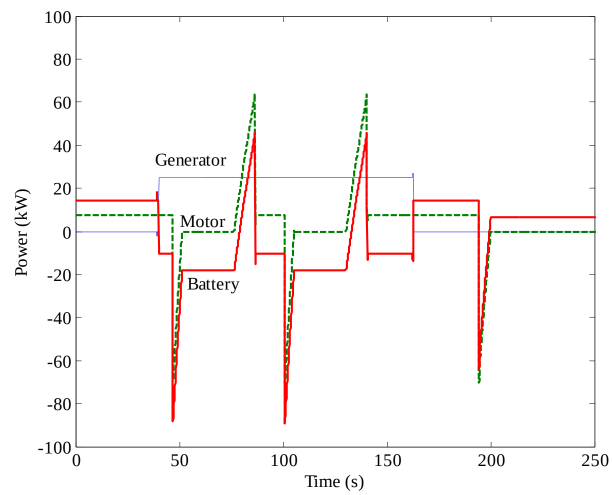

Figure 13. H_2ICE-flywheel shuttle bus powers

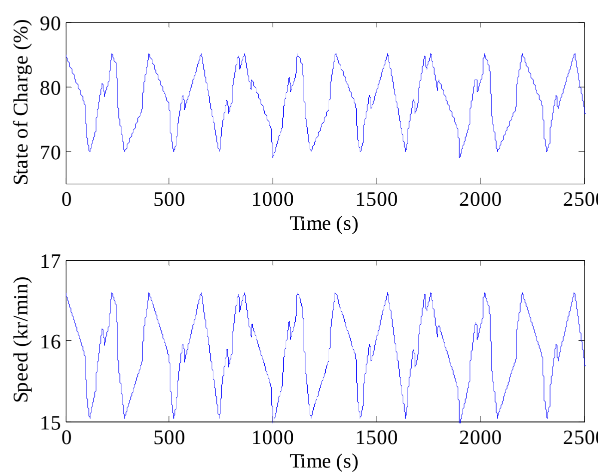

Figure 14. Flywheel state of charge and speed for H_2ICE-flywheel shuttle

TABLE II
SHUTTLE BUS SIMULATION SUMMARY

Parameter	Fuel Cell-Battery	Fuel Cell-Flywheel	H_2ICE-Battery	H_2ICE-Flywheel	Unit
Vehicle Mass	8845	6122	8873	6150	kg
Range with Hydrogen	298	370	225	275	km
Range without Hydrogen	49	2.2	39	2.1	km
Total Range	347	372.2	264	277.1	km
Vehicle Energy Consumption	1.78	1.43	2.37	1.94	kWh/km
Prime Mover Average Efficiency	46.7	47.4	35.2	35.2	%
Combined H_2ICE-Generator Average Efficiency	N/A	N/A	33.0	33.0	%
Percentage of Recoverable Braking Energy Recuperated	48.7	69.9	48.6	69.6	%
Acceleration Time from 0 to 11.2 m/s	13.2	8.9	13.2	8.9	s

the larger energy storage content of the battery system is heavily underutilized. The net effect is a battery system that is more than 2700 kg more massive than the flywheel system, has a reduced efficiency, shorter life, increased maintenance needs, and leads to comparatively higher vehicle fuel consumption.

Flywheel storage systems excel in such vehicular applications as they allow the storage system designer to tailor power capability and energy storage independently and thus avoid over designing either parameter. In this regard, the flywheel system discussed was designed to meet the energy storage needs of the shuttle while simultaneously using its higher power density advantage and improved efficiency to achieve a significantly lower mass system resulting in superior shuttle bus performance and fuel consumption.

REFERENCES

[1] A. Emadi, S.S. Williamson, "Fuel Cell Vehicles: Opportunity and Challenges," IEEE Power Engineering Society General Meeting, vol. 2, pp. 1640-1645, June 2004.

[2] A.F. Burke, M. Miller, "Fuel Efficiency Comparison of Advanced Hybrid Transit Buses using Fuel Cell and Engine Hybrid Electric Drivelines," AIAA 35th Intersociety Energy Conversion Engineering Conference and Exhibit, July 2000.

[3] T. Yokoyama, Y. Naganuma, "Development of Fuel-Cell Hybrid Bus," SAE World Congress, 2003-01-0417, March 2003.

[4] M.C. Péra, D. Hissel, J.M. Kaufmann, "Fuel Cell Systems for Electric Vehicles," IEEE 55th Vehicular Technology Conference vol. 4, pp.2097-2102, May 2002.

[5] US Department of Energy, EERE, Hydrogen, Fuel Cells, and Infrastructure Technologies Program, Types of Fuel Cells, [Online] http://www.eere.energy.gov/hydrogenandfuelcells/fuelcells/fc_types.html.

[6] M. Sasaki, et al. "Development of a Hybrid Capacitor System for Urban Buses," JSAE Review, vol. 23, num. 4, pp. 451-457, Oct. 2002.

[7] Ford Touts its Shuttle Buses as Hydrogen-Powered Future, Tom Krisher; *Austin American Statesman*, July 11, 2007.

[8] X. Tang, D.M. Kabat, R.J. Natkin, W.F. Stockhausen, "Ford P2000 Hydrogen Engine Dynamometer Development," SAE World Congress, 2002-01-0242, March 2002.

[9] C.M. White, R.R. Steeper, and A.E. Lutz, "The Hydrogen Fueled Internal Combustion Engine – A Technical Review," *International Journal of Hydrogen Energy*, vol. 31, pp. 1292-1305, 2006.

[10] J.W. Heffel, "NO_x Emission and Performance Data for a Hydrogen Fueled Internal Combustion Engine at 1500 RPM Using Exhaust Gas Recirculation," *International Journal of Hydrogen Energy*, vol. 28, pp. 901-908, 2003.

[11] M. Berkmüller, H. Rottengruber, A. Eder, N. Brehn, G. Elässer, G. Müller-Alander, C. Schwarz, "Potentials of a Charged SI-Hydrogen Engine," SAE Powertrain and Fluid Systems Conference and Exhibition, 2003-01-3210, Oct. 2003.

[12] H. Rottengruber, M. Berkmüller, G. Elässer, N. Brehn, and C. Schwarz, "Direct Injection Hydrogen SI-Engine Operation Strategy and Power Density Potentials," SAE Powertrain and Fluid Systems Conference and Exhibition, 2004-01-2927, Oct. 2004.

[13] J. Fiene, T. Braithwaite, R. Boehm, Y. Baghzouz, T. Kell, "Development of a Hydrogen Engine for a Hybrid Electric Bus," SAE World Congress, 2002-01-1085, March 2002.

[14] C. S. Hearn, M.M. Flynn, M.C. Lewis, R.C. Thompson, R.G. Longoria, "Low Cost Flywheel Energy Storage for a Fuel Cell Powered Transit Bus," IEEE Vehicular Power and Propulsion Conference, Sept. 2007.